RSC Advances

PAPER

View Article Online
View Journal | View Issue

Cite this: *RSC Adv.*, 2020, **10**, 29821

3D printing of milk-based product

Cheng Pau Lee,[ab] Rahul Karyappa[bc] and Michinao Hashimoto *[abc]

We developed a method to perform direct ink writing (DIW) three-dimensional (3D) printing of milk products at room temperature by changing the rheological properties of the printing ink. 3D printing of food products has been demonstrated by different methods such as selective laser sintering (SLS) and hot-melt extrusion. Methods requiring high temperatures are, however, not suitable to creating 3D models consisting of temperature-sensitive nutrients. Milk is an example of such foods rich in nutrients such as calcium and protein that would be temperature sensitive. Cold-extrusion is an alternative method of 3D printing, but it requires the addition of rheology modifiers and the optimization of the multiple components. To address this limitation, we demonstrated DIW 3D printing of milk by cold-extrusion with a simple formulation of the milk ink. Our method relies on only one milk product (powdered milk). We formulated 70 w/w% milk ink and successfully fabricated complex 3D structures. Extending our method, we demonstrated multi-material printing and created food with various edible materials. Given the versatility of the demonstrated method, we envision that cold extrusion of food inks will be applied in creating nutritious and visually appealing food, with potential applications in formulating foods with various needs for nutrition and materials properties, where food inks could be extruded at room temperature without compromising the nutrients that would be degraded at elevated temperatures.

Received 7th June 2020
Accepted 2nd July 2020

DOI: 10.1039/d0ra05035k

rsc.li/rsc-advances

Introduction

This paper describes a method to perform 3D printing of milk-based products using a direct ink writing (DIW) 3D printer by changing the rheological properties of the printing ink (that we termed milk inks). We applied this method to 3D-print milk ink formulated from commercially available milk powders without additives. The formulated milk inks were in the form of pastes at room temperature. While previous work has shown 3D printing of milk with additives such as xanthan gum,[1] our work focused on the formulation of 3D printable milk inks with minimum additives. To this end, the ink studied in this work entirely consisted of powdered milk and water. We studied the effect of the concentration of the milk powders on the rheological properties of the milk inks and the printability of the milk inks by DIW 3D printing. We successfully 3D-printed structures with inks containing 70–75 w/w% of milk powders.

3D printing allows layer-by-layer fabrication of 3D structures using materials specific to the mechanism of printing, ranging from thermoplastics and hydrogels.[2–4] This technology is applied across diverse fields of engineering, including bio-printing to create new organs,[5,6] metal printing to create aeroplane parts,[7] concrete printing to construct houses[8] and materials printing to create electronic devices[9] and microfluidic devices.[10,11] Food printing is one of the emerging applications;[12,13] 3D food printing allows customizing nutrients based on individual needs,[14,15] fabricating aesthetically pleasing food,[16] and modifying internal structures of the food.[17] Different mechanisms of 3D printing have been demonstrated for food printing; selective laser sintering (SLS) applies a laser to melt and fuse powder particles. In SLS, the printable materials are limited to those based on sugars and fats to ensure thermal fusion by laser sintering.[18] Alternatively, extrusion-based methods have been widely used in food printing because of their flexibility to dispense liquid-based food materials.[19–21] Hot-melt extrusion has been one of the most widely-used methods of extrusion-based food.[22] Methods such as hot-melt extrusion and SLS are not always suitable to model temperature-sensitive food, however, because they require the elevated temperature to melt food samples. For example, milk is rich in nutrients such as calcium and protein that would be temperature sensitive, and not compatible with the process involving high temperature.

Cold extrusion requires food additives to alter the rheological properties of the food ink.[23,24] In cold extrusion, 3D printing relies solely on the rheology of ink. The viscosity, yield stress, and storage modulus of the ink are essential parameters for DIW to determine the printability and structure integrity of the printed structures. Additives are commonly included in food

[a]*Pillar of Engineering Product Development, Singapore University of Technology and Design, 8 Somapah Rd, Singapore 487372, Singapore. E-mail: hashimoto@sutd.edu.sg*
[b]*SUTD-MIT International Design Centre (IDC), Singapore University of Technology and Design, 8 Somapah Rd, Singapore 487372, Singapore*
[c]*Digital Manufacturing and Design (DManD) Centre, Singapore University of Technology and Design, 8 Somapah Rd, Singapore 487372, Singapore*

ink to alter the rheological properties for cold extrusion. In one work, researchers added xanthan gum and k-carrageenan gum into mashed potatoes to print self-supporting structures.[25] Alternatively, researchers added glycerol, xanthan gum, and whey protein isolate with milk powder to facilitate printing.[1] These works involved the use of additives to maintain the fidelity of the printed structures. As such, there are increasing interests to 3D-print temperature sensitive food materials *via* cold extrusion. Currently available food inks for cold extrusion contain multiple additives with pre-identified concentrations, which entails complexity that requires judicious optimization to achieve the printability.

To overcome the challenges to 3D-print temperature sensitive food, we demonstrated cold extrusion of food inks *via* simple alternation of rheological properties without extensive use of additives. We selected a milk product as an example of our demonstration. The formulated milk ink is based on a single milk-based ingredient that controls the rheological properties of its own ink. To the best of our knowledge, demonstration of 3D printing of milk without additional rheological modifiers at room temperature has not been shown. The rheological properties of milk ink were modified by adjusting the concentration of milk powder, which was characterized and evaluated for the printability. With inks containing 70–75 w/w% of milk powders, we successfully printed complex 3D structures. Extending the demonstration, we achieved multi-material printing with milk ink and other edible inks. The principles and methods presented here should be applicable to other edible inks for the DIW 3D printing at room temperature, which should find a wide range of applications in the customized fabrication of food products by 3D printing. Our work demonstrated a simple way to modify the rheology of food inks. We believe this capability will contribute to unlock full potential of 3D printing of foods such as customization of texture and personalization of nutrition.

Results and discussion

Rheological characterization of milk ink

3D food printing is commonly demonstrated with the hot-melt extrusion that requires temperature-sensitive food material such as chocolate.[26] In this work, we use milk as an example to demonstrate cold extrusion (Fig. 1). Understanding the rheology of the materials is critical to determine the printability of the ink by cold extrusion.[27] A printable ink should exhibit shear-thinning behavior, where the viscosity is low at a high shear rate to allow extrusion of ink from the nozzle. It has been reported that inks with viscosity more than 100 Pa s were printed using a DIW printer.[28,29] We initially studied the rheological properties of the formulated inks. The values of the viscosity of milk ink with different concentrations (10–75 w/w%, denoting 10 w/w% as M10, *etc.*) were plotted as a function of shear rate (Fig. 2A and Table 1). The addition of milk powder increased the viscosity of the inks from 0.51 ± 0.46 Pa s (M10) to 46 291.77 ± 5626.42 Pa s (M75). The viscosity of M60, M65, M70, and M75 decreased as the shear rate increased, suggesting that the formulated milk inks were shear-thinning and pseudoplastic fluids. The yield stress of the ink is a crucial parameter in DIW 3D printing; it is the minimum shear stress required to initiate flow; the flow of the ink suggested the loss of the cohesion among the colloidal particles due to van der Waals interactions.[30] As the concentration of milk powder increased, the yield stress also increased from 0.01 ± 0 Pa (M10) to 330.57 ± 23.64 Pa (M75). The increase in yield stress implied that the colloidal network within the ink was enhanced as the concentration of milk powder increased. The mesh structures printed using inks of M10, M60, and M65 spread due to low yield stress (0.01 ± 0 Pa for M10, 11.15 ± 2.21 Pa for M60, 78.23 ± 5.57 Pa for M65) (Fig. 3). The mesh structures printed using inks of M70 and M75 were maintained due to high yield stress (105.95 ± 13.21 Pa for M70 and 330.57 ± 23.64 Pa for M75) (Fig. 3). These observations suggested that a high value of yield stress allowed maintaining the printed structures of the materials.

To understand the degree of non-Newtonian characteristics, the Herschel–Bulkley model was applied to describe the rheological behavior of the formulated milk inks.[31]

$$\sigma = \sigma_y + K\dot{\gamma}^n$$

$$\log_{10}(\sigma - \sigma_y) = \log_{10}K + n\log_{10}\dot{\gamma}$$

The shear-rate and shear-stress were subjected to curve fitting to Herschel–Bulkley model to obtain flow behavior index (n) and flow consistency index (K) where n indicates the degree of non-Newtonian characteristics of the fluid and K indicates the degree of viscosity of the fluid. $n < 1$ indicates that the fluid exhibits shear thinning behavior, and $n > 1$ indicates that the fluid exhibits shear thickening behavior. $n = 1$ indicates that the fluid is a Newtonian

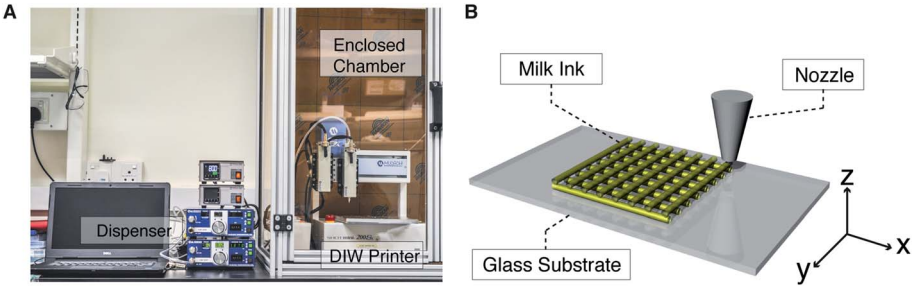

Fig. 1 A setup for direct ink writing (DIW) 3D printing for cold extrusion. (A) A photograph of a DIW printer used in the experiment. (B) A schematic illustration of DIW of mesh structure with milk ink onto a glass substrate.

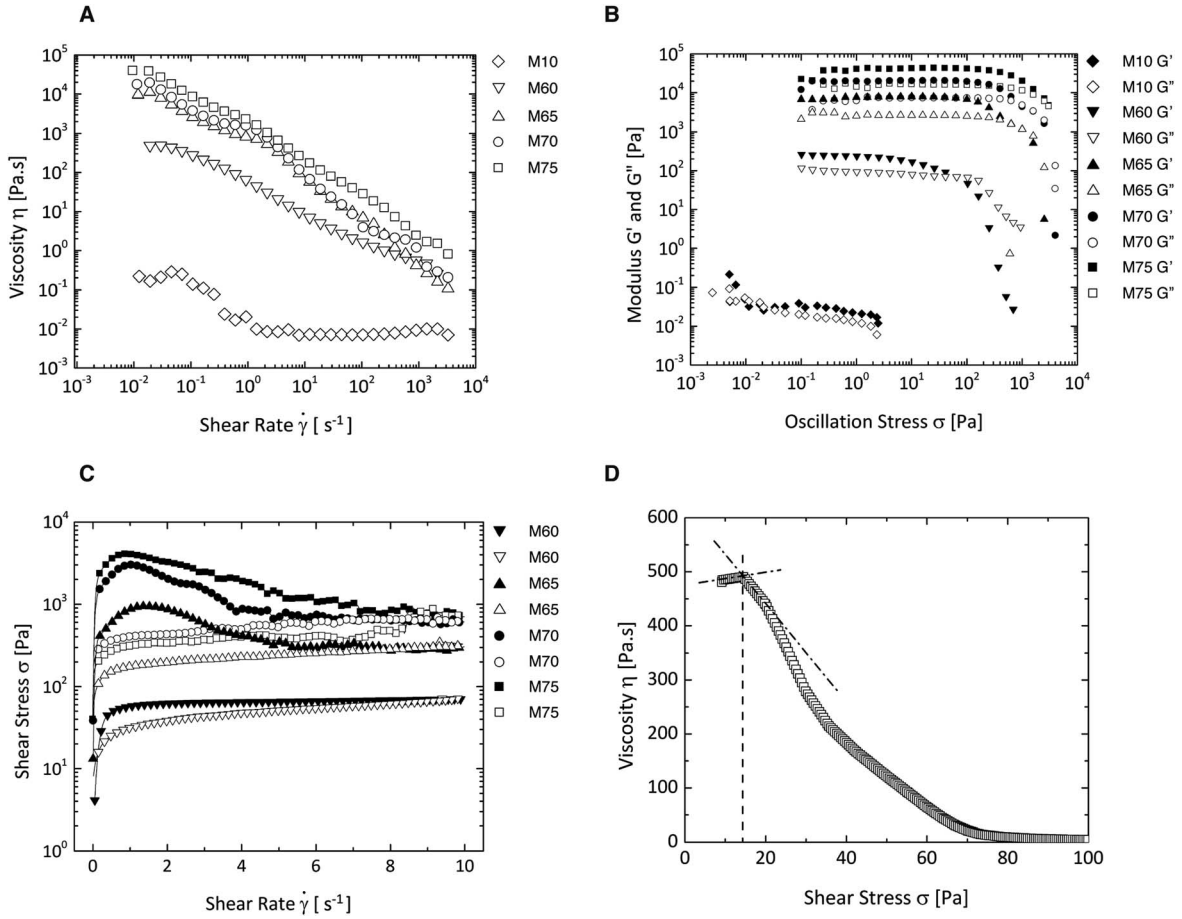

Fig. 2 Rheological characterization of the milk ink (10–75 w/w%; 10 w/w% was denoted as M10, *etc.*). (A) Viscosity (μ) as a function of applied shear rate ($\dot{\gamma}$). (B) Storage moduli (G') and loss moduli (G'') as a function of applied oscillatory shear stress (σ). (C) Thixotropic loop test measuring the shear stress (σ) as a function of increasing (solid symbols) and decreasing (open symbols) shear rates ($\dot{\gamma}$). (D) Stress ramp test for ink M60 to determine its yield stress at 25 °C.

fluid. Yield stress (σ_y) was taken as the intersection point of the two tangent lines, one in the linear region of viscosity and the other where viscosity decreased drastically (Fig. 2D). The K and n were obtained by plotting $\log_{10}(\sigma - \sigma_y)$ against $\log_{10}\dot{\gamma}$ and fitting the best linear line; the y-intercept of the line was the value of n, and the gradient was the value of K. The values of n were all less than 1 (Table 1), indicating that all formulated milk inks exhibited shear-thinning behavior. The values of n of M10 were 0.86 ± 0.12; this value was close to the value of 1, indicating that it had a low degree of shear-thinning behavior. The low yield stress of ink of M10 (0.01 ± 0 Pa) caused leakage of ink from the nozzle. As the concentration of the milk powders increased, K also increased. The increase of K suggested increased mechanical strength of the ink at rest to hold the printed structures,[32] which ensured the printability of the ink.

Oscillation amplitude tests were performed to determine the storage modulus (G') and loss modulus (G''). These values allowed us to understand the viscoelastic property of the ink matrix. We observed that G' lay on the plateau in the linear viscoelastic region (LVR) (Fig. 2B). In this region, the colloidal network within the ink remained intact due to their elastic behavior. The G' in this region is a measure of mechanical strength at rest, which is a critical parameter that determines the structural integrity of the printed material after deposition. As the concentration of milk powder increased, G' increased

Table 1 Yield stress and parameters of Herschel–Bulkley model of milk inks with different concentrations. All values were calculated as means (±standard deviations)

Sample	M10	M60	M65	M70	M75
Viscosity μ [Pa s]	0.51 ± 0.46	438.26 ± 64.59	11 528.53 ± 486.25	19 374.37 ± 1443.11	46 291.77 ± 5626.42
Yield stress σ_y [Pa]	0.01 ± 0	11.15 ± 2.21	78.23 ± 5.57	105.95 ± 13.21	330.57 ± 23.64
Flow behavior index n	0.86 ± 0.12	0.35 ± 0.01	0.56 ± 0.03	0.64 ± 0.12	0.50 ± 0.07
Consistency index K [Pa s^n]	0.02 ± 0.01	37.07 ± 1.46	422.01 ± 56.95	950.10 ± 125.06	2702.13 ± 723.88

Table 2 Oscillatory amplitude sweep test results tested at 25 °C. All values were calculated as means (±standard deviations)

Sample	M10	M60	M65	M70	M75
Storage modulus G' [Pa]	—	187.86 ± 105.81	7131.80 ± 346.12	18 894.33 ± 2942.75	47 843.67 ± 11 612.42
Crossover stress $G' = G''$ [Pa]	—	56.21 ± 31.28	631.23 ± 2.68	921.09 ± 34.55	3692.31 ± 337.39
Critical stress σ_c [Pa]	—	4.10 ± 0.09	63.13 ± 0	100.01 ± 0	251.19 ± 0.01

Table 3 Thixotropic parameters for the milk inks with different concentrations tested at 25 °C. All values were calculated as means (±standard deviations)

Sample	M10	M60	M65	M70	M75
Thixotropic loop area [Pa s^{-1}]	—	165.73 ± 57.33	2701.76 ± 462.77	6027.87 ± 376.78	16 084.94 ± 2145.34

from 56.21 ± 31.28 Pa (M60) to 3692.31 ± 337.39 Pa (M75) (Table 2). The higher G' suggested the stronger bonds and the higher printability of the ink. The values of G' were higher than the values of G'' for all milk inks except M10. This observation indicated that the milk inks possessed solid-like behaviors, which allowed the printed material to retain its shape.

Finally, thixotropic loop tests were performed to understand the time-dependent breakdown and recovery of the microstructure of the milk inks. The inbound area between the ascending and descending curve of the thixotropy loop was measured as the scale of thixotropy (Fig. 2C).[33] The addition of milk powder increased the thixotropy loop area from 165.73 ± 57.33 Pa s^{-1} (M60) to 16 084.94 ± 2145.34 Pa s^{-1} (M75) (Table 3). We observed less spreading of printed mesh structures as the concentration of milk ink increased (Fig. 3). The reduced spreading of the ink suggested improved recovery of the colloidal network within the ink, which suggested that the degree of thixotropy increased with the increase in the concentration of the milk powder.

Printability of milk ink

In DIW 3D printing, the desirable ink should have two characteristics: (1) exhibiting shear-thinning behavior and (2) maintaining its shape upon deposition. We confirmed that the values of n of the ink were less than 1 to ensure shear-thinning characteristics (Table 1). At the same time, the same ink should have high yield stress and storage modulus to ensure the printed material to retain its shape and maintaining structural integrity. In order to verify the printability of the inks, we printed mesh structures. The low yield stress of ink of M10 caused the ink to yield to the gravitational force, and the ink leaked from the nozzle without applied pressure. Thus, the ink of M10 was not suitable to form defined layers and to create 3D models. The mesh structures printed using inks of M10, M60, and M65 spread due to low yield stress (Fig. 3). The mesh structures printed using inks of M70 and M75 were maintained due to high yield stress (Fig. 3). M70 was less viscous than M75; under similar printing conditions, M70 was extruded more smoothly than M75, which was apparent from discontinuous edges of the printed structures. While this paper focused on characterizing rheological properties of different milk inks, other parameters such as (1) dispensing pressure, (2) nozzle velocity, and (3) nozzle diameter were also essential to determine the amount of the food inks extruded from the moving nozzle and achieve the print fidelity.

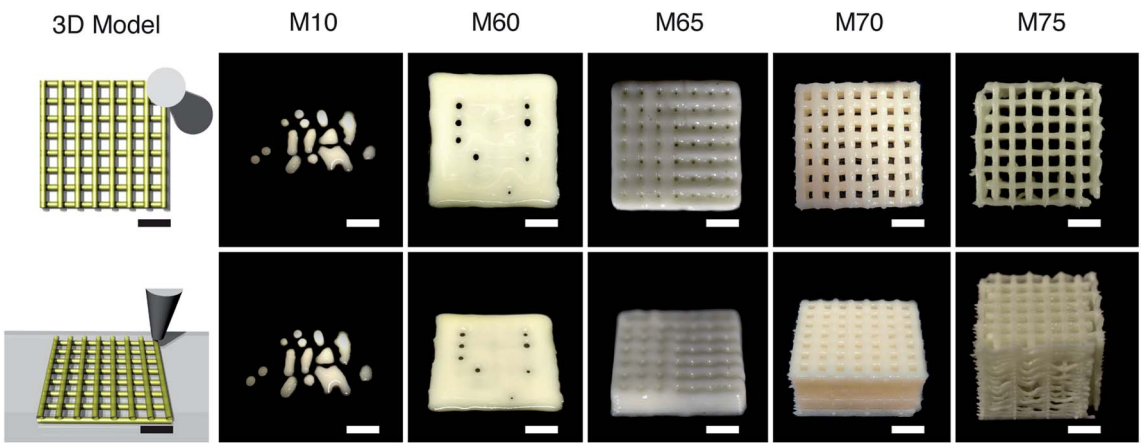

Fig. 3 Optical images of the DIW 3D-printed models of milk. The effects of the concentration of milk on the spreading of the printed ink were evident from the printed models. The mesh structures printed with inks of M10, M60, and M65 spread and filled the gaps. The printed mesh structures were maintained after printing with M70 and M75 (all scale bar: 5 mm).

These observations suggested that M70 and M75 were the candidates to perform 3D printing of complex structures (Fig. 4). We fabricated 3D model of a couch using inks of M65, M70, and M75 (Fig. 4A). The structure printed with ink M65 was not able to hold its shape due to low yield stress and storage modulus. The structures printed with ink M70 and M75 were able to hold its shape due to high yield stress and storage modulus. Both inks were suitable to create 3D structures, while the yield stress and storage modulus of M70 were sufficient to allow the printed structure to hold its shape. We printed other geometries with the ink of M70, and the structures were able to support itself without deforming (Fig. 4B–D). We note that M70 required less pressure than M75 for extrusion (because M70 was less viscous than M75), which would be practically preferred

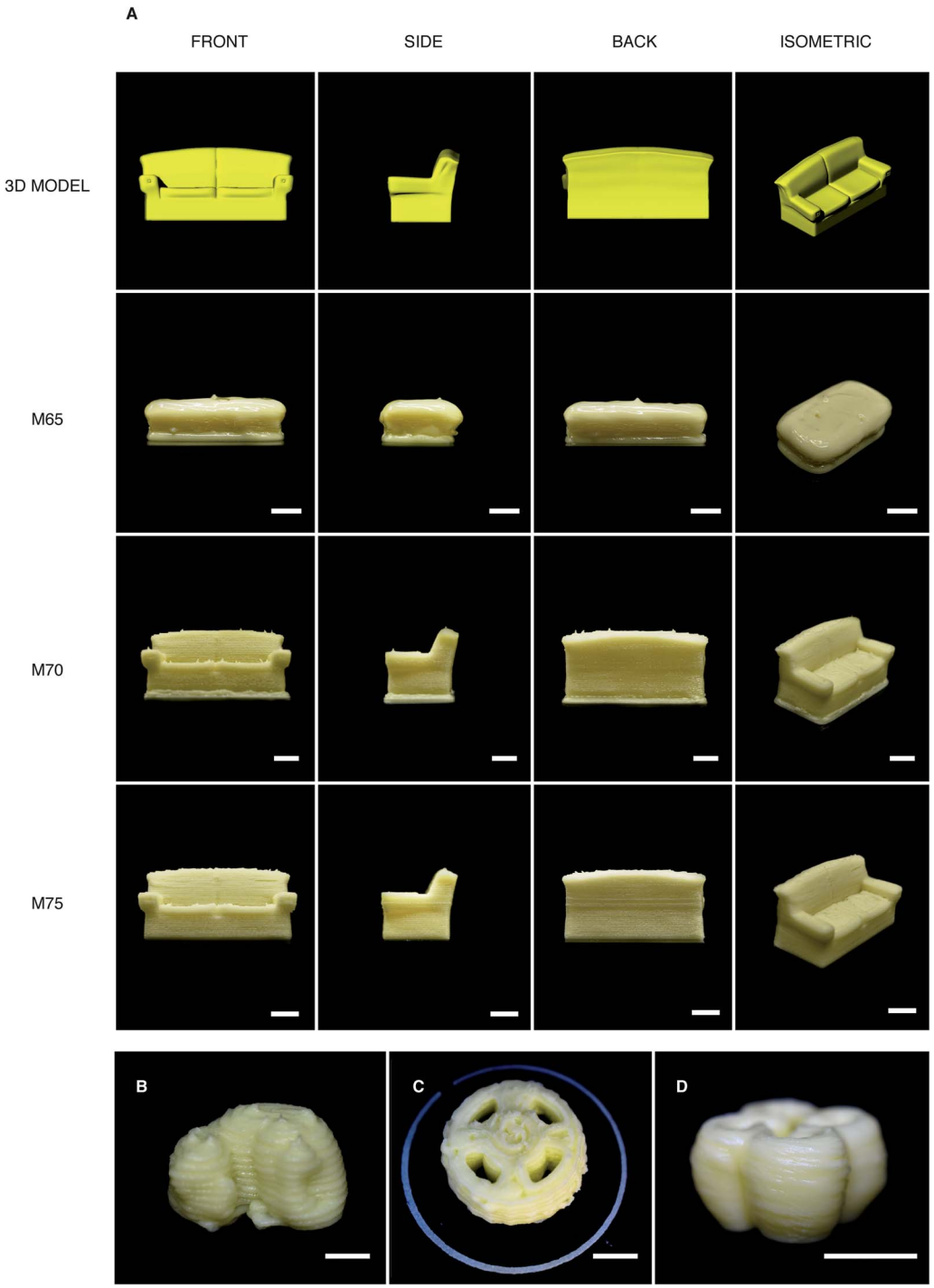

Fig. 4 Optical images of the 3D printed complex structures. (A) Front, side, back, and isometric views of the 3D models and printed structures with inks of M60, M70, and M75. (B–D) Printed structures of the fortress, wheel, and cloverleaf, respectively, with the ink of M70 (all scale bar: 5 mm).

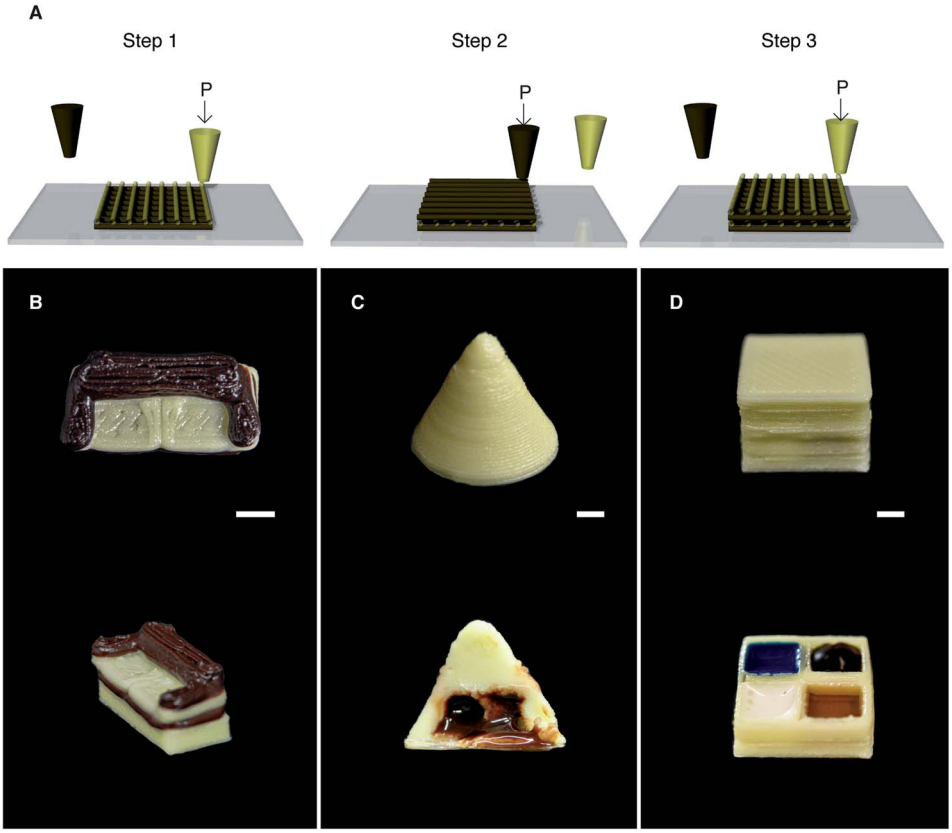

Fig. 5 3D-printed multi-food models. (A) Schematic illustration of multi-material DIW 3D printing. (B) 3D structure of a couch printed with milk and chocolate inks at different layers. (C) 3D printed cone containing liquid chocolate syrup as an internal filling. (D) 3D printed cube with four compartments containing liquid blueberry syrup, liquid chocolate syrup, milk cream, maple syrup as internal fillings (all scale bar: 5 mm).

when the operation of the instrument was limited to certain pressure. Overall, the use of milk powder without additional additive was demonstrated to formulate 3D-printable food inks *via* cold extrusion.

Multi-food printing

Finally, we demonstrated multi-material printing using the DIW printer equipped with two independent syringes. A schematic illustration of the multi-food printing is shown (Fig. 5A). In multi-food printing, 3D models were was printed using multiple syringes containing different food inks. We demonstrated printing a 3D structure of a couch with milk ink and chocolate inks at different layers (Fig. 5B). The first few layers were printed with the milk ink, followed by a few layers with the chocolate ink. The subsequent layers were printed with the milk ink again. The rheology of the printable chocolate inks were studied in the previous work.[24] Alternatively, 3D printing of the structures containing different fillings was demonstrated (Fig. 5B and C). In this demonstration, we used the inks of chocolate, coconut, maple syrup, and blueberry as the internal fillings. We produced a 3D model with a rigid enclosure and soft fillings to provide different textures. In this fabrication, we printed the bottom layers of the 3D structures with voids using milk ink. Next, the voids were filled with different inks using other syringes. Finally, the top layers were printed to close the voids. All inks used in this demonstration possessed different rheological properties while we did not perform the rheological characterization of the food inks that were used as filling. Those inks were stably enclosed within the patterns created by M70, the rheology-modified milk ink. Overall, our method of food 3D printing was readily extended to multi-food printing to create 3D models with materials possessing various rheological properties.

Conclusions

We discussed 3D printing of milk-based materials using a DIW 3D printer. 3D printable milk inks were formulated without additional rheological modifiers, and 3D structures were fabricated *via* cold extrusion using a DIW 3D printer at room temperature. We performed rheological characterization to determine (1) viscosity, (2) yield stress, and (3) storage modulus of the inks. Milk ink with 70 w/w% milk powder was suitable for DIW 3D printing with a yield stress of 105.95 $\pm$ 13.21 Pa and a storage modulus of 18 894.33 $\pm$ 2942.75 Pa. The formulated ink was shear-thinning, with $n < 1$ in Herschel–Bulkley model, and capable of maintaining structural integrity upon deposition. We also demonstrated multi-material printing with milk ink and other edible inks. This method offered an easy route to formulate other edible inks without additives and fabricate

a visually appealing meal without temperature control. Our method has potential applications in formulating foods with various needs for nutrition and materials properties, where food inks could be extruded at room temperature without compromising the nutrients that would be degraded at elevated temperatures.

Experimental section/materials and methods

Preparation of milk ink

Materials used were commercially available milk powder (Fernleaf Family Milk, Fonterra, Malaysia) and deionized (DI) water. The samples of the milk ink were prepared by adding milk powder into deionized water at different weight concentrations (M10, M60, M65, M70, and M75; 10 w/w% is denoted as M10 and *etc.*). The chocolate ink used in multi-food printing was formulated by mixing 20 w/w% of cocoa powder (Hershey's Cocoa, Hershey, USA) with chocolate syrup (Hershey's Syrup, Hershey, USA). Samples were then mixed thoroughly and degassed with Thinky Mixer (ARE-250, Thinky Corporation, Tokyo, Japan) at 25 °C. Other materials used in multi-material printing included maple syrup (Great Northern Pure Organic Maple Syrup, Foodsterr, Canada), blueberry syrup (Great Northern Organic Blueberry Maple Syrup, Foodsterr, Canada) and milk cream (Fresh Cream, Amul, India), all of which were used as purchased.

Rheological characterization

The measurement of the rheology of the ink was performed with an oscillatory rheometer (Discovery Hybrid Rheometer DHR-2, TA Instruments, Delaware, USA). Parallel plates consisting of stainless steel with a diameter of 40 mm and a truncation gap of 1000 μm were used for all measurements. Viscosity tests were conducted by applying a stepwise shear rate ramp for 0.1–2000 s^{-1}. The stress sweep measurements were conducted with a logarithmically increasing shear stress at a constant frequency of 1 Hz over the range of 0.1–4000 Pa to determine the viscoelastic properties of the samples. Thixotropy loop tests were conducted with a logarithmically increasing shear rate over the range of 0.0001–10 s^{-1} and then returned with a logarithmically decreasing shear rate to the initial shear rate. Prior to the test, all excess material outside the plate was removed to prevent the edge effects. All rheological measurements were conducted at 25 ± 0.1 °C on triplicate samples.

DIW 3D printing

3D printing was performed using a pneumatic DIW printer (SHOTmini 200 Sx, Musashi Engineering, Inc., Tokyo Japan). MuCAD V (Musashi Engineering, Inc., Tokyo, Japan) software was used in conjunction with the DIW printer to control the toolpath and speed of the nozzle. The DIW printer was enclosed in a chamber to maintain a sterile environment. 3D models were obtained from Thingiverse, a public repository of 3D printable models, or designed on Solidworks (Dassault Systèmes, Waltham, MA, USA). 3D model designed on Solidworks was then converted to stereolithography (STL) file format in the software itself, while the 3D model obtained from Thingiverse was downloaded in the STL format. The STL model was imported to Slic3r, an open-source software that slices model, into 200–500 μm thick layers. The software generated G-code for 3D printing. G-code was converted to MuCAD V code *via* a script written in Python and loaded to the DIW printer. All samples were loaded into a 50 mL luer-lock dispensing barrel fitted with the nozzles of the fixed diameters (22–27 G, Birmingham gauge). The barrel was then placed onto the syringe holder on the DIW printer. The substrates used in this work were glass substrates. Prior to printing, the standoff distance between the substrate and nozzle was calibrated to the layer thickness, 200–500 μm, depending on the viscosity of the milk ink. A height feeler gauge was used to control the standoff distance accurately. The printer was programmed manually to lower the nozzle until the tip touched the height feeler gauge. The printing speed and dispensing pressure were also calibrated according to the viscosity of the milk ink. All printings were performed at room temperature.

Conflicts of interest

There are no conflicts to declare.

Acknowledgements

C. P. L. acknowledged the financial support from the President's Graduate Fellowship awarded by Ministry of Education (MOE), Singapore. The authors thank International Design Centre (IDC) at Singapore University of Technology and Design (SUTD) for the project support (IDG11700103; Digital Fabrication of Edible Materials) and SUTD Growth Plan (SGP) in Healthcare Research (SGPHCRS1907; Thrust 3-3 3D Food Printing).

References

1 Y. Liu, D. Liu, G. Wei, Y. Ma, B. Bhandari and P. Zhou, *Innovative Food Sci. Emerging Technol.*, 2018, **49**, 116–126.
2 R. Karyappa, A. Ohno and M. Hashimoto, *Mater. Horiz.*, 2019, **6**, 1834–1844.
3 P. F. Flowers, C. Reyes, S. Ye, M. J. Kim and B. J. Wiley, *Addit. Manuf.*, 2017, **18**, 156–163.
4 C. B. Highley, C. B. Rodell and J. A. Burdick, *Adv. Mater.*, 2015, **27**, 5075–5079.
5 X. Wang, Q. Ao, X. Tian, J. Fan, H. Tong, W. Hou and S. Bai, *Polymers*, 2017, **9**, 401.
6 N. Noor, A. Shapira, R. Edri, I. Gal, L. Wertheim and T. Dvir, *Adv. Sci.*, 2019, **6**, 1900344.
7 A. A. Shapiro, J. P. Borgonia, Q. N. Chen, R. P. Dillon, B. McEnerney, R. Polit-Casillas and L. Soloway, *J. Spacecr. Rockets*, 2016, **53**, 952–959.
8 C. Gosselin, R. Duballet, P. Roux, N. Gaudillière, J. Dirrenberger and P. Morel, *Mater. Des.*, 2016, **100**, 102–109.
9 S. R. Shin, R. Farzad, A. Tamayol, V. Manoharan, P. Mostafalu, Y. S. Zhang, M. Akbari, S. M. Jung, D. Kim,

M. Comotto, N. Annabi, F. E. Al-Hazmi, M. R. Dokmeci and A. Khademhosseini, *Adv. Mater.*, 2016, **28**, 3280–3289.
10 T. Ching, Y. Li, R. Karyappa, A. Ohno, Y.-C. Toh and M. Hashimoto, *Sens. Actuators, B*, 2019, **297**, 126609.
11 W. H. Goh and M. Hashimoto, *Macromol. Mater. Eng.*, 2018, **303**, 1700484.
12 S. L. Voon, J. An, G. Wong, Y. Zhang and C. K. Chua, *Virtual Phys. Prototyp.*, 2019, **14**, 203–218.
13 C. Tan, C. K. Chua, L. Li and G. Wong *3rd Intl. Conf. on Progress in Additive Manufacturing*, 2018, DOI: 10.25341/D42C7V.
14 A. Derossi, R. Caporizzi, D. Azzollini and C. Severini, *J. Food Eng.*, 2018, **220**, 65–75.
15 J. Sun, Z. Peng, L. Yan, J. Fuh and G. S. Hong, *Int. J. Bioprint.*, 2015, **1**(1), 27–38.
16 I. Dankar, A. Haddarah, F. E. L. Omar, F. Sepulcre and M. Pujolà, *Trends Food Sci. Technol.*, 2018, **75**, 231–242.
17 Z. Liu, B. Bhandari, S. Prakash and M. Zhang, *Food Res. Int.*, 2018, **111**, 534–543.
18 J. V. Diaz, B. K. J. C. Van, M. W. J. Noort, J. Henket and P. Bri€er, *US Pat.* 10092030B2, 2018.
19 M. Lille, A. Nurmela, E. Nordlund, S. Metsä-Kortelainen and N. Sozer, *J. Food Eng.*, 2018, **220**, 20–27.
20 L. Wang, M. Zhang, B. Bhandari and C. Yang, *J. Food Eng.*, 2018, **220**, 101–108.
21 C. Tan, W. Y. Toh, G. Wong and L. Lin, *Int. J. Bioprint.*, 2018, **4**(2), 143.
22 L. Hao, S. Mellor, O. Seaman, J. Henderson, N. Sewell and M. Sloan, *Virtual Phys. Prototyp.*, 2010, **5**, 57–64.
23 A. Gholamipour-Shirazi, I. T. Norton and T. Mills, *Food Hydrocolloids*, 2019, **95**, 161–167.
24 R. Karyappa and M. Hashimoto, *Sci. Rep.*, 2019, **9**, 14178.
25 Z. Liu, M. Zhang and C.-h. Yang, *LWT*, 2018, **96**, 589–596.
26 S. Mantihal, S. Prakash, F. C. Godoi and B. Bhandari, *Innovative Food Sci. Emerging Technol.*, 2017, **44**, 21–29.
27 F. C. Godoi, S. Prakash and B. R. Bhandari, *J. Food Eng.*, 2016, **179**, 44–54.
28 R. L. Truby and J. A. Lewis, *Nature*, 2016, **540**, 371–378.
29 B. A. Aguado, W. Mulyasasmita, J. Su, K. J. Lampe and S. C. Heilshorn, *Tissue Eng., Part A*, 2012, **18**, 806–815.
30 A. Sun and S. Gunasekaran, *Int. J. Food Prop.*, 2009, **12**, 70–101.
31 W. H. Herschel and R. Bulkley, *Kolloid-Z.*, 1926, **39**, 291–300.
32 W. J. Costakis, L. M. Rueschhoff, A. I. Diaz-Cano, J. P. Youngblood and R. W. Trice, *J. Eur. Ceram. Soc.*, 2016, **36**, 3249–3256.
33 M. V. Ghica, M. Hirjau, D. Lupuleasa and C. E. Dinu-Pirvu, *Molecules*, 2016, **21**, 786.

